THE JOURNAL OF BIOLOGICAL CHEMISTRY VOL. 283, NO. 32, pp. 21978–21987, August 8, 2008

Metabolomic and Mass Isotopomer Analysis of Liver Gluconeogenesis and Citric Acid Cycle

*I. INTERRELATION BETWEEN GLUCONEOGENESIS AND CATAPLEROSIS; FORMATION OF METHOXAMATES FROM AMINOOXYACETATE AND KETOACIDS**

Received for publication, May 6, 2008, and in revised form, June 9, 2008 Published, JBC Papers in Press, June 10, 2008, DOI 10.1074/jbc.M803454200

Lili Yang[‡], Rajan S. Kombu[‡], Takhar Kasumov[‡], Shu-Han Zhu[‡], Andrea V. Cendrowski[‡], France David[‡], Vernon E. Anderson[§], Joanne K. Kelleher[¶], and Henri Brunengraber[‡1]

From the Departments of [‡]Nutrition and [§]Biochemistry, Case Western Reserve University, Cleveland, Ohio 44106 and the [¶]Department of Chemical Engineering, Massachusetts Institute of Technology, Cambridge, Massachusetts 02154

We conducted a study coupling metabolomics and mass isotopomer analysis of liver gluconeogenesis and citric acid cycle. Rat livers were perfused with lactate or pyruvate ± aminooxyacetate or mercaptopicolinate in the presence of 40% enriched $NaH^{13}CO_3$. Other livers were perfused with dimethyl [1,4-$^{13}C_2$]succinate ± mercaptopicolinate. In this first of two companion articles, we show that a substantial fraction of gluconeogenic carbon leaves the liver as citric acid cycle intermediates, mostly α-ketoglutarate. The efflux of gluconeogenic carbon ranges from 10 to 200% of the rate of liver gluconeogenesis. This cataplerotic efflux of gluconeogenic carbon may contribute to renal gluconeogenesis *in vivo*. Multiple crossover analyses of concentrations of gluconeogenic intermediates and redox measurements expand previous reports on the regulation of gluconeogenesis and the effects of inhibitors. We also demonstrate the formation of adducts from the condensation, in the liver, of (i) aminooxyacetate with pyruvate, α-ketoglutarate, and oxaloacetate and (ii) mercaptopicolinate and pyruvate. These adducts may exert metabolic effects unrelated to their effect on gluconeogenesis.

Although hypothesis-based research is the gold standard of biological investigation, it is necessary from time to time to expand its scope by a period of data-based discovery research. The current omic revolution is fulfilling this need. By widening the knowledge base, omics and in particular metabolomics (1–5) identify unknown correlations, allowing the formulation and testing of new hypotheses. We hypothesized that the scope of metabolomics could be enhanced by associating it with mass isotopomer analysis, a powerful technique developed over the past 16 years (reviewed in Refs. 6, 7). This association would allow the identification of unexpected labeling patterns of metabolites, pointing to unknown reactions and/or regulatory mechanisms (8). We used this association of techniques to expand our previous studies on the influence of metabolic zonation of the liver on the labeling patterns of metabolites and on metabolic rates calculated from these labeling patterns.

Over the past 12 years, questions were raised on the potential influence of the metabolic zonation of the liver (9) on the ^{13}C-labeling pattern of glucose released by gluconeogenesis (GNG),[2] glycogenolysis, or both. The zonated structure of the liver results in translobular gradients of enzyme activities and of blood substrate concentrations (glycerol, acetate, and NH_4^+) (10–12). Also, the computation of the mass isotopomer distribution (MID) of (i) glucose labeled from [^{13}C]glycerol or (ii) fatty acids and sterols labeled from [^{13}C]acetate revealed the occurrence of translobular gradients of enrichment of triose phosphates or lipogenic acetyl-CoA, respectively (10, 13, 14). This results in underestimations of fractional rates of glucose, fatty acid, and sterol synthesis calculated from the MID of these compounds synthesized from a ^{13}C-labeled substrate. In this study, we hypothesized that the metabolic zonation of the liver might result in incompatible labeling of intermediates extracted from the whole liver. Such incompatibilities were suggested in 1970 by Veneziale *et al.* (15). In livers perfused with [2-^{14}C]pyruvate and quinolinate, an inhibitor of phosphoenolpyruvate carboxykinase (PEPCK), they observed substantial differences in the labeling of PEP and 3-phosphoglycerate. We also hypothesized that the extra-mitochondrial metabolism of citric acid cycle (CAC) intermediates would affect their labeling pattern and result in differences in the labeling patterns of tissue and extracellular metabolites. We tested these hypotheses by combining metabolomics with the determination of MIDs of gluconeogenic and CAC intermediates.

We perfused rat livers with ^{13}C-substrates, the label of which is channeled to [1-^{13}C]PEP before entering GNG. One substrate was $NaH^{13}CO_3$, which labels liver GNG from lactate or pyruvate via carboxylation and isotopic exchange reactions

* This work was supported, in whole or in part, by National Institutes of Health Metabolomics Roadmap Initiative Grant R33DK070291. This work was also supported by the Cleveland Mt. Sinai Health Care Foundation. The costs of publication of this article were defrayed in part by the payment of page charges. This article must therefore be hereby marked "*advertisement*" in accordance with 18 U.S.C. Section 1734 solely to indicate this fact.

[1] To whom correspondence should be addressed: Dept. of Nutrition, Case Western Reserve University School of Medicine-WG48, 10900 Euclid Ave., Cleveland, OH 44106-4954. Tel.: 216-368-6548; Fax: 216-368-6560; E-mail: hxb8@case.edu.

[2] The abbreviations used are: GNG, gluconeogenesis; αGP, α-glycerophosphate; AOA, aminooxyacetate; DHAP, dihydroxyacetone phosphate; CAC, citric acid cycle; MID, mass isotopomer distribution; MPA, mercaptopicolinate; OAA, oxaloacetate; PEP, phosphoenolpyruvate; PEPCK, phosphoenolpyruvate carboxykinase; TMS, trimethylsilyl; GC-MS, gas chromatography-mass spectrometry; LC-MS/MS, liquid chromatography-tandem mass spectrometry; HPLC, high pressure liquid chromatography.

(16). The second substrate was dimethyl [1,4-$^{13}C_2$]succinate, which labels PEP via reactions of the citric acid cycle and PEPCK. We modulated the rates of GNG from lactate, pyruvate, or [1,4-$^{13}C_2$]succinate using mercaptopicolinate (MPA), an inhibitor of PEPCK (17, 18), or aminooxyacetate (AOA), an inhibitor of the glutamate-aspartate shuttle (19–21). In this first of two companion articles, we show that a substantial fraction of gluconeogenic carbon leaves the liver as α-ketoglutarate and other CAC intermediates. Also our data reveal the formation of methoxamates from AOA and ketoacids.

EXPERIMENTAL PROCEDURES

Materials—General chemicals, biochemicals, and enzymes were obtained from Sigma. Mercaptopicolinic acid was obtained from Apin Chemical Ltd. (UK), and pentafluorobenzyl bromide was from Pierce. [$^{13}C_6$]Citric, [1,5-$^{13}C_2$]citric, and [$^{13}C_4$]succinic acids, phosphoenol[1-^{13}C]pyruvate (99%), K^{13}CN (99%), [$^2H_5$]glycerol, ^2H_2O, and NaO^{2}H (98%) were purchased from Isotec (Miamisburg, OH). [1,4-$^{13}C_2$]Succinic acid (99%) and NaB$^2H_4$ (99%) were purchased from Cambridge Isotope Laboratories. An internal standard of (*RS*)-3-hydroxy-[$^2H_5$]glutarate was prepared by isotopic exchange of acetone dicarboxylic diethyl ester in ^2H_2O and NaO^{2}H, followed by reduction with NaB$^2H_4$, and extraction in acid. This procedure is similar to that previously used for the preparation of (*RS*)-3-hydroxy-[$^2H_5$]butyrate from acetoacetate (22). [6-^{13}C]Citric acid was prepared by reacting acetone dicarboxylic diethyl ester with K^{13}CN, followed by hydrolysis of the nitrile. The purity of the synthesized compounds was assessed by GC-MS of trimethylsilyl (TMS) derivatives. Dimethyl [1,4-$^{13}C_2$]succinate was prepared by reacting the acid with excess diazomethane. The purified product did not contain any detectable monoester or free acid. Reference standards of [$^{13}C_3$]glycerophosphate, dihydroxy-[$^{13}C_3$]acetone phosphate, and [$^{13}C_3$]glyceraldehyde-3-phosphate were prepared from [$^{13}C_3$]glycerol using glycerol kinase, α-glycerophosphate (αGP) dehydrogenase, and triosephosphate isomerase. The carboxymethoxamates of pyruvate, OAA, and α-ketoglutarate were prepared as described by Borek and Clarke (23) for pyruvate carboxymethoxamate. Their purity was confirmed by ammonia-positive chemical ionization GC-MS of the TMS derivatives. The mercaptopicolinate-pyruvate hemithioacetal was prepared by reacting mercaptopicolinate and sodium pyruvate at neutral pH in degassed water for 6 h. The adduct was extracted with diethyl ether, converted to its TMS derivative, and assayed by ammonia-positive chemical ionization GC-MS. The m/z = 460 of the M + 1 molecular ion was shifted to m/z = 463 when the synthesis was conducted with [$^{13}C_3$]pyruvate. However, attempts at isolating a pure product were unsuccessful because of the instability of the adduct, which decomposes readily to its constituents.

Liver Perfusion Experiments—Sprague-Dawley male rats were kept for 8–12 days on Teklad F6 rodent chow *ad libitum*. Livers from 18-h fasted rats (180–220 g) were first perfused (24) for 10 min with nonrecirculating bicarbonate buffer (40 ml/min) containing unlabeled substrate. Then they were perfused with buffer containing (i) 40% enriched NaH$^{13}CO_3$ and 5 mM lactate, or 2 mM pyruvate ± 0.3 mM MPA, or 0.5 mM AOA (protocol I), or (ii) dimethyl [1,4-$^{13}C_2$]succinate ± 0.3 mM MPA (protocol II). In orientation experiments, we found that the labeling of gluconeogenic and CAC intermediates, as well as glucose production, were two to four times greater with dimethyl [1,4-$^{13}C_2$]succinate than with [1,4-$^{13}C_2$]succinate (not shown). Similar ratios in glucose production from dimethylsuccinate and succinate were reported by Rognstad (25). Therefore, we conducted all the experiments of this group with 0.5 mM dimethyl [1,4-$^{13}C_2$]succinate ± 0.3 mM MPA. Because the mercaptopicolinate molecule contains a free SH group, we wanted to avoid the possibility of oxidation in the perfusate gassed with 95% O_2 + 5% CO_2. Therefore, MPA was infused into the liver perfusion line via a syringe pump. At 30 min (protocol I) or 20 min (protocol II), the livers were quick-frozen and kept in liquid N_2 until analyzed.

Sample Preparation—Powdered frozen tissue (1.5 g), spiked with internal standards (150 nmol of [$^{13}C_6$]citrate, 100 nmol of [$^{13}C_4$]succinate, and 50 nmol of (*RS*)-3-hydroxy-[$^2H_5$]glutarate), was extracted with 19 ml of chloroform/methanol, 2:1, pre-cooled at −25 °C, using a Polytron homogenizer. During the 5-min extraction, the tube was partially immersed in acetone kept at −25 °C by periodic addition of dry ice. Then 6 ml of ice-cold water was added to the tube, and the extraction (Folch wash (26)) was continued for 5 min. The slurry was centrifuged at 670 × *g* for 20 min at 4 °C. The upper methanol/water phase was collected and treated with 200 μmol of methoxylamine-HCl to protect ketoacids. The lower chloroform phase was vortexed for 5 min with 10 ml of methanol/water, 3:2, pre-cooled at −20 °C. After the 20-min centrifugation, the two upper methanol/water phases were combined, adjusted to pH 8.0 with NaOH, and evaporated in a Savant vacuum centrifuge. The residue was reacted with 100 μl of *N*,*O*-bis(trimethylsilyl)trifluoroacetamide with 10% trimethylchlorosilane (Regisil) at 70 °C for 50 min to form the TMS and methoxamate-TMS derivatives of the analytes.

GC-MS Assays—Analyses were carried out on an Agilent 5973 mass spectrometer, linked to a model 6890 gas chromatograph equipped with an autosampler, a Varian VF-5MS capillary column (60 m, 0.25 mm inner diameter), and an EZ guard column (10 m). The carrier gas was helium (1 ml/min) with a pulse pressure of 40 p.s.i. The injection was either 1 μl split 10:1 or 2 μl splitless. The injector temperature was set at 270 °C and the transfer line at 280 °C. The GC temperature program was as follows: start at 80 °C, hold for 1 min, increase by 10 °C/min to 320 °C, hold at 320 °C for 5 min. The ion source and the quadrupole were set at 150 °C. The ammonia pressure was adjusted to optimize peak areas. For each analyte, we monitored the signals at the nominal m/z (M0) and at all detectable naturally labeled mass isotopomers (M1, M2, M3). The MID of each analyte was compared with the theoretical distribution. The electron ionization fragmentation pattern of analytes was introduced in the National Institute of Science and Technology (NIST) software to help with the identification and to detect interferences. The relative concentrations and MIDs of compounds of interest, identified during electron ionization runs, were assayed under ammonia positive chemical ionization conditions. Retention times and m/z monitored are listed in Ref. 27.

LC-MS/MS Assays—Electrospray-ionization mass spectrometry of AOA adducts were performed on a 4000 QTrap

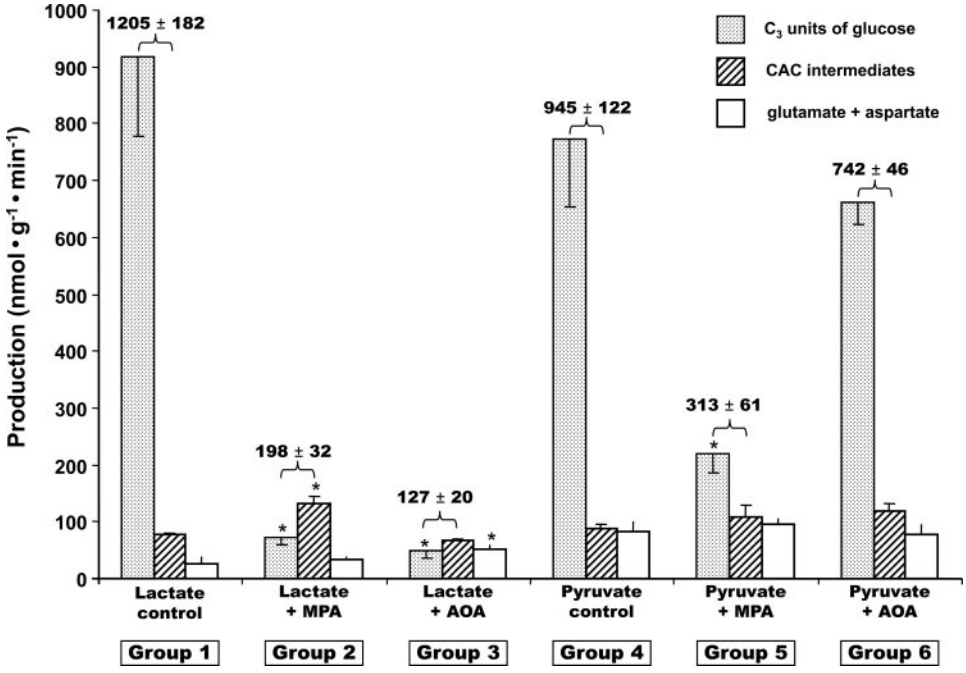

FIGURE 1. **Glucose production (*grey bars*, in C_3 units), release of citric acid cycle intermediates (*hatched bars*), and release of glutamate + aspartate (*white bars*) in livers were perfused with buffer containing 40% $NaH^{13}CO_3$, 5 mM lactate, or 2 mM pyruvate ± 0. 3 mM mercaptopicolinate, or ± 0.5 mM aminooxyacetate.** The *numbers above* each pair of *grey* and *hatched bars* represent a minimal rate of pyruvate carboxylation. Data are presented as mean ± S.E. ($n = 4–7$).

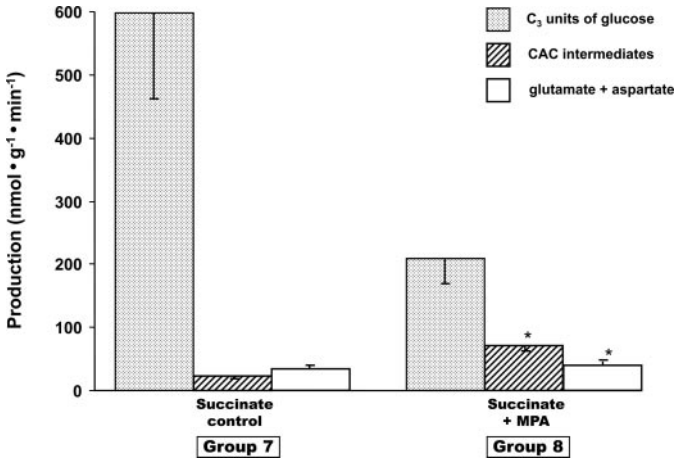

FIGURE 2. **Glucose production (*grey bars*, in C_3 units), release of citric acid cycle intermediates (*hatched bars*), and release of glutamate + aspartate (*white bars*) in livers were perfused with buffer containing [1,4-$^{13}C_2$]succinate ± 0. 3 mM mercaptopicolinate.** Data are presented as mean ± S.E. ($n = 4–6$).

mass spectrometer (Applied Biosystems, Foster City, CA) coupled to an Agilent 1100 HPLC system. The ion source was maintained at 500 °C under nitrogen nebulization at a pressure of 70 p.s.i. The heater gas (nitrogen) was at a pressure of 70 p.s.i. The curtain gas pressure was 35 p.s.i., and the collision-activated dissociation gas pressure was held at high; turbo ion spray voltage was −4,500 V. Declustering potential was −25 V; entrance potential was −10 V; collision energy was −5 V for enhanced mass spectra scans; collision cell exit potential was −11 V; and channel electron multiplier was 2,400 V. The multiple reaction monitoring pairs monitored were *m/z* 159.9 → 75.1 for pyruvate-AOA (CE −13), *m/z* 86.9 → 59.0 for pyruvate (CE −12), *m/z* 217.9 → 75.1 for α-ketoglutarate-AOA (CE −13), *m/z* 145.0 → 100.9 for α-ketoglutarate (CE −13), *m/z* 204.0 → 75.1 for OAA-AOA (CE −15), *m/z* 130.9 → 86.9 for OAA (CE −12), and *m/z* 90.0 → 57.9 for AOA (CE −28), with a dwell time of 40 ms. Analyst software (version 1.4.1; Applied Biosystems) was used for data registration and calibration.

The autosampler cooler was maintained at 6 °C. The analyses were performed on an Aquasil C18 column (250 × 4 mm, 5 μm particle size; Thermo Electron Corp.) maintained at 40 °C. Mobile phase A was 5 mM ammonium formate (pH 8.0, adjusted with ammonia):acetonitrile (95:5, v/v). Mobile phase B was acetonitrile. For elution, initially mobile phase A was held at 100% with a starting flow rate of 0.35 ml/min for 6 min. By 1 min the aqueous phase was brought down to 25% A and a flow rate of 0.5 ml/min and held for 1 min. Finally the gradient was brought back to 100% mobile phase A and was held for 4 min for equilibration at a flow rate of 0.5 ml/min.

Calculations—The relative concentrations of metabolites (inhibitor *versus* control) were calculated (24) as shown in Equation 1,

$$\frac{\text{average of ((area analyte)/(area ref. compound))}_i}{\text{average of ((area analyte)/(area ref. compound))}_c} \quad \text{(Eq. 1)}$$

where subscripts *i* and *c* represent the intervention and control group, respectively; ref. indicates reference. The formula was used to calculate relative concentrations (inhibitor *versus* control group).

Statistics—Data are presented as mean ± S.E. Significance was tested by independent sample *t* test with SPSS software. Statistical significance was set for $p < 0.05$.

RESULTS AND DISCUSSION

Our studies were conducted in four directions, *i.e.* (i) flux measurements (glucose production and release of CAC intermediates (Figs. 1 and 2)); (ii) redox indicators reflecting the [NADH]/[NAD^+]ratios; (iii) comparisons of metabolite profiles by crossover analysis (28) of metabolomic data expressed as relative concentrations (Figs. 3–6); and (iv) search for adducts of ketoacids and aminooxyacetate or mercaptopicolinate (Fig. 7).

Interrelation between GNG, Loss of CAC Intermediates, and Pyruvate Carboxylation—Fig. 1 shows data from groups 1–6 (perfusions with lactate or pyruvate ± MPA or AOA). Each cluster of three bars shows glucose production (in nanomoles of

$C_3 \cdot min^{-1} \cdot g^{-1}$), total release of CAC intermediates, and total release of glutamate + aspartate (in nanomoles$\cdot min^{-1} \cdot g^{-1}$). The releases of CAC intermediates, glutamate and aspartate, are detailed in Table 1. Fig. 2 shows the corresponding data for groups 7 and 8 (perfusions with dimethyl [1,4-$^{13}C_2$]succinate ± MPA). The rates of glucose production confirm previous data as follows: (i) inhibition of GNG from lactate, pyruvate, or succinate by MPA (18), and (ii) inhibition of GNG from lactate, but not pyruvate, by AOA (19, 20). Unexpectedly, in all cases (Figs. 1 and 2), the livers released CAC intermediates, of which 70% or more was α-ketoglutarate (Table 1). The other CAC intermediates released were, in decreasing order of abundance, malate, succinate, fumarate, and citrate. The livers also released glutamate (no glutamine) and aspartate, which reflect the release of CAC intermediates and proteolysis. In some cases, the release of CAC intermediates + glutamate + aspartate increased as a result of the inhibition of GNG (groups 2 and 8 *versus* 1 and 7). However, under all conditions, part of the gluconeogenic carbon left the liver as compounds, which, under *in vivo* conditions, are excreted in urine and/or are converted to glucose in the kidney (29). This suggests the existence of a liver-to-kidney traffic of gluconeogenic anions. Such traffic may explain why mice lacking liver PEPCK have normal glycemia and glucose turnover (30). In these mice, compensatory renal GNG is presumably fueled in part by cataplerotic gluconeogenic intermediates released by the liver.

A minimum rate of pyruvate carboxylation can be calculated, in perfusions with lactate or pyruvate (Fig. 1), by adding the rates of glucose production (in C_3 units) and the releases of CAC intermediates (as indicated in Fig. 1 by *numbers above* the first two bars of each set). A maximal rate of pyruvate carboxylation can be calculated as the sum of glucose production, release of CAC intermediates, and release of glutamate + aspartate. One cannot distinguish the production of glutamate and aspartate derived from proteolysis *versus* release of CAC intermediates. Although the labeling of glutamate and aspartate from $NaH^{13}CO_3$ was substantial, such labeling could have occurred by isotopic equilibration of amino acids derived from proteolysis with OAA and α-ketoglutarate (more on this below and in the accompanying article (41)). In any case, pyruvate carboxylation exceeded GNG by at least 10% in the absence of inhibitor (Fig. 1, *groups 1* and *4*) and by up to 200% in the presence of an inhibitor (Fig. 1, *groups 2, 3, 5,* and *6*).

Although MPA inhibits PEPCK fairly specifically, its inhibition of GNG from lactate or pyruvate led to 6- and 3-fold decreases, respectively, in pyruvate carboxylation (Fig. 1). This effect resulted probably from the accumulation of OAA (Fig. 4, *B* and *C*, to be discussed below). In contrast, AOA had very different effects on pyruvate carboxylation in experiments with lactate (84% decrease from controls) *versus* pyruvate (no significant change from controls). It is likely that, in some of the conditions tested, the inhibition of GNG by MPA and/or AOA led to a decrease in the uptake of the gluconeogenic precursor lactate or pyruvate. The uptake of the precursors could not be measured in

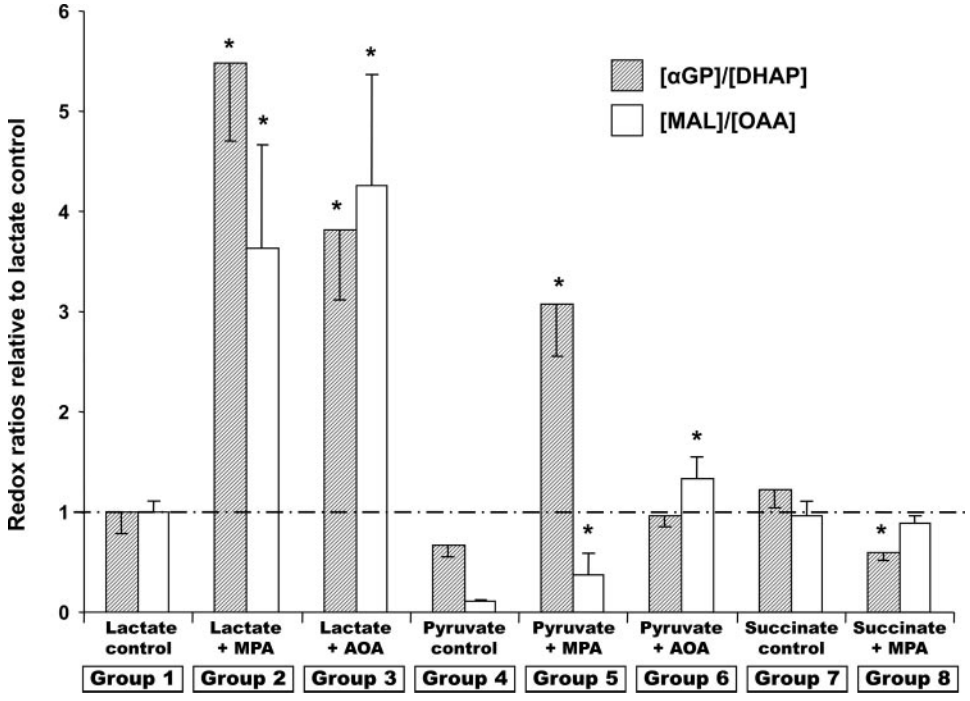

FIGURE 3. **Relative redox ratios [αGP]/[DHAP] (*hatched bars*) and [malate]/[OAA] (*white bars*) in perfused livers.** The ratios, calculated as described under "Experimental Procedures," are expressed relative to the corresponding ratio of the lactate control group set to 100%.

TABLE 1

Release of CAC intermediates, aspartate, and glutamate from perfused rat livers

Each group of livers was perfused with nonrecirculating buffer containing the substrate ± inhibitor indicated in the left column. Succinate was used as its dimethyl ester. Data are presented as nmol$\cdot g^{-1} \cdot min^{-1}$ (mean ± S.E.; $n = 5$). The total release of intermediates is shown in Fig. 1.

Substrate ± inhibitor	Succinate	Fumarate	Malate	αKG	Citrate	Glutamate	Aspartate
5 mM lactate control	1.6 ± 0.7	−0.5	7.5 ± 0.3	69.1 ± 1.5	0.01 ± 0.1	26.8 ± 11.1	−0.03
5 mM lactate + 0.3 mM MPA	4.0 ± 0.6	−0.4	7.5 ± 0.4	55.6 ± 1.6	0.2 ± 0.2	32.5 ± 6.8	0.1 ± 0.2
5 mM lactate + 0.5 mM AOA	6.3 ± 2.8	5.4 ± 1.5	9.9 ± 0.9	108.4 ± 10.9	0.5 ± 0.1	34.2 ± 9.7	18.1 ± 3.4
2 mM pyruvate control	1.6 ± 0.7	−0.2	6.4 ± 0.6	81.0 ± 6.7	0.3 ± 0.04	82.4 ± 16.8	0.3 ± 0.0
2 mM pyruvate + 0.3 mM MPA	4.6 ± 0.6	2.5 ± 0.9	5.8 ± 0.5	94.9 ± 16.9	0.9 ± 0.2	94.5 ± 10.4	1.1 ± 0.1
2 mM pyruvate + 0.5 mM AOA	1.9 ± 0.4	−0.1	5.2 ± 0.2	112.8 ± 9.6	0.2 ± 0.05	76.1 ± 16.4	2.0 ± 0.8
0.5 mM dimethyl succinate control	9.3 ± 2.7	0.6 ± 0.1	5.6 ± 0.3	4.9 ± 1.8	2.9 ± 0.4	35.0 ± 6.0	1.0 ± 0.6
0.5 mM dimethyl succinate + 0.3 mM MPA	4.5 ± 1.0	6.2 ± 0.9	14.8 ± 0.8	30.0 ± 5.1	12.8 ± 2.1	40.6 ± 5.6	0.2 ± 0.2

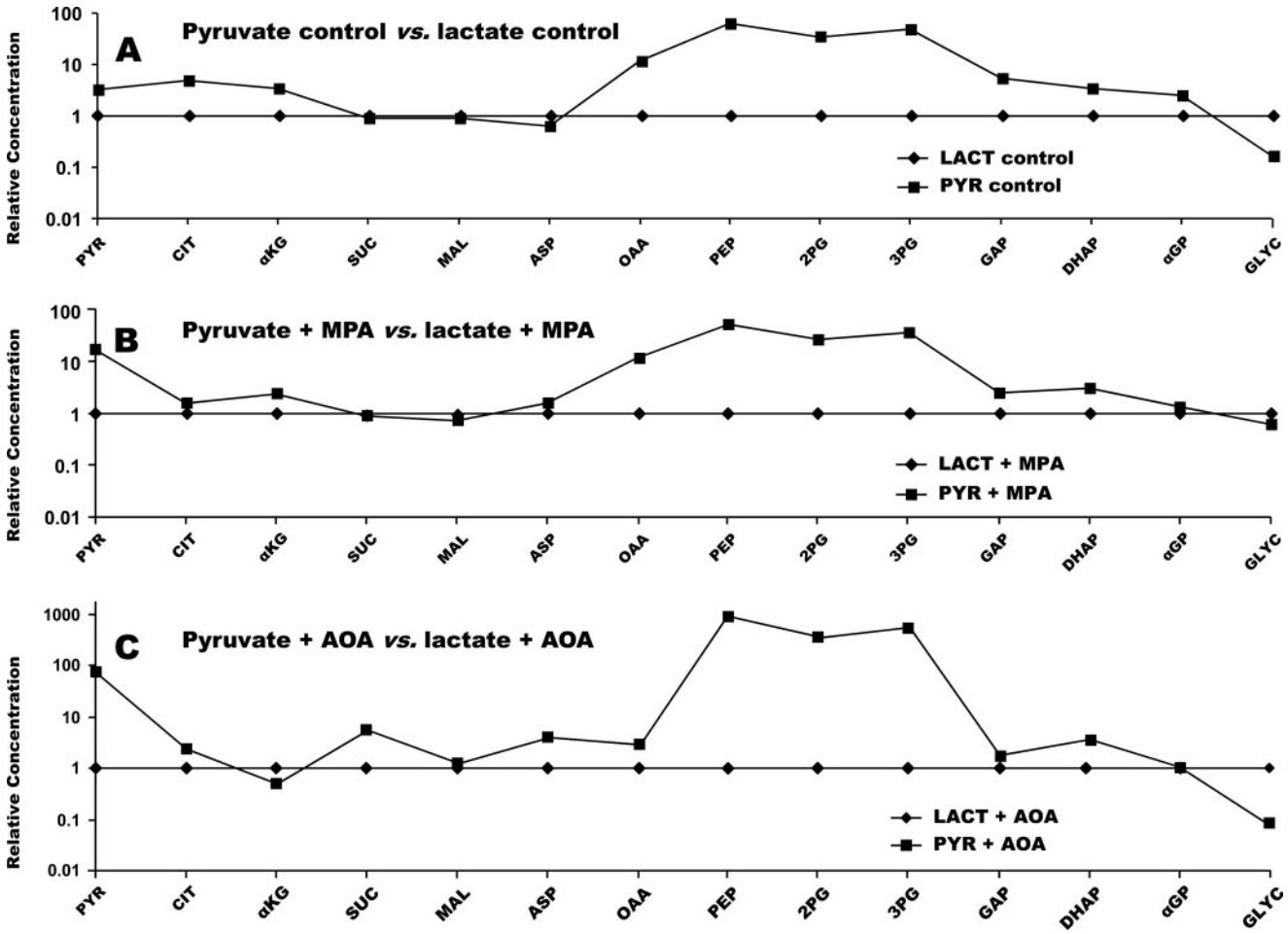

FIGURE 4. **Crossover plots comparing the concentration of gluconeogenic and citric acid cycle intermediates in livers perfused with 2 mM pyruvate *versus* 5 mM lactate.** *A*, base-line conditions. *B*, +0.3 mM MPA. *C*, +0.5 mM AOA. *C* was redrawn with modifications from Fig. 3 of Ref. 27. *CIT*, citrate; *MAL*, malate; *SUC*, succinate; *ASP*, aspartate; *2PG*, 2-P-glycerate; *3PG*, 3-P-glycerate; *GLYC*, glycerate; *LACT*, lactate.

our nonrecirculating perfusions with fairly high concentrations of precursors. In conclusion, when GNG is inhibited, the modulation of pyruvate carboxylation and of the release of CAC intermediates is a multifactorial process that requires further investigation.

Redox and Crossover Analyses of Metabolomic Data—Determining the relative concentrations of metabolites (inhibitor groups *versus* corresponding control groups) allowed calculating two relative redox ratios (Fig. 3) and performing a number of crossover analyses (28) (Figs. 4–7), which confirm and expand previous studies. The tissue [αGP]/[DHAP] ratio reflects the [NADH]/[NAD^+] ratio in the cytosol if the activity of αGP dehydrogenase is sufficient to equilibrate the cytosolic [αGP]/[DHAP] and [NADH]/[NAD^+] pools. The tissue [malate]/[OAA] ratio reflects a composite of the cytosolic and mitochondrial [NADH]/[NAD^+] ratios.

We were unable to measure the [β-hydroxybutyrate]/[acetoacetate] ratio, which reflects the mitochondrial [NADH]/[NAD^+] ratio, because of the very low abundance of acetoacetate. The relative redox ratios shown in Fig. 3 are expressed in relation to the ratios of the lactate control group taken as 100%. The interpretation of these relative redox ratios must take into account the following. (i) They are computed from the GC-MS areas of reduced and oxidized substrates in two groups of perfusions (one of them the lactate control group, see "Experimental Procedures"). (ii) In some cases, the areas of the oxidized substrate (DHAP and OAA) are very small. (iii) Hepatic lipolysis leads to the formation of αGP, which may not fully equilibrate with DHAP (see Ref. 41). Consider first the [αGP]/[DHAP] relative ratios. Inhibition of GNG from lactate by MPA or AOA markedly increased the [NADH]/[NAD^+] ratio in the cytosol (Fig. 3). In both cases, glucose production from lactate was inhibited. Thus, the cytosolic NADH formed by lactate dehydrogenase was not re-oxidized by glyceraldehyde-3-phosphate dehydrogenase. The increase in the cytosolic [NADH]/[NAD^+] ratio led to a decrease in the concentration of pyruvate (Fig. 5*C* and Fig. 6*C*). This decrease probably (i) reflects a decrease in the conversion of lactate to pyruvate, and (ii) contributed to the inhibition of GNG by MPA. Increases in the cytosolic [NADH]/[NAD^+] ratio, reflected by increases in the [lactate]/[pyruvate] ratio, in the presence of MPA or AOA had been previously reported in *in vivo* livers (17) and in isolated hepatocytes, respectively (20). The increase in the [malate]/[OAA] ratio probably reflects the cytosolic malate/OAA couple, because the production of mitochondrial OAA was not impaired by MPA or AOA.

In perfusions with pyruvate, the carbon skeleton of OAA is transferred from mitochondria to cytosol as malate, carrying

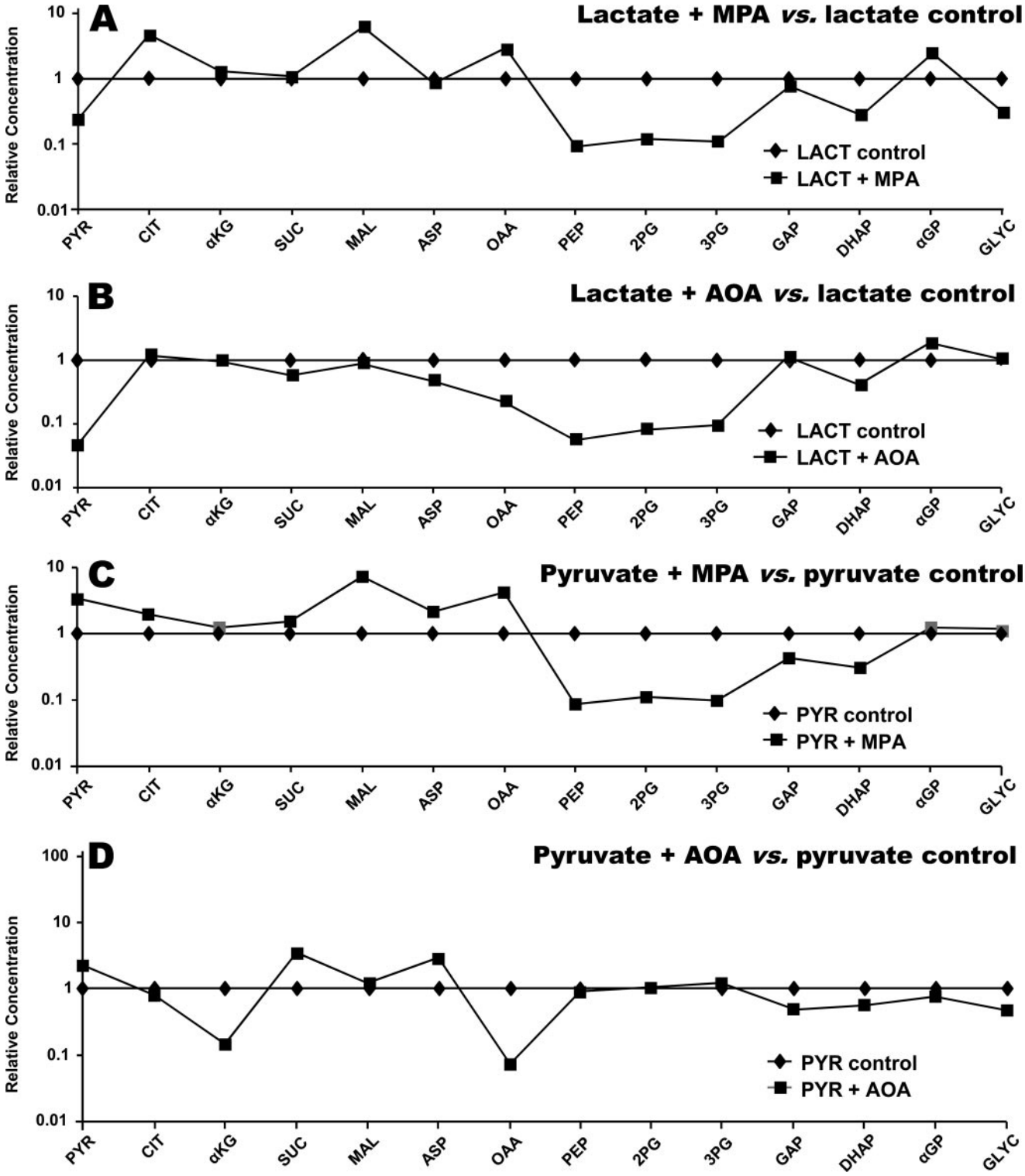

FIGURE 5. **Crossover plots comparing the effects of 0.3 mM MPA or 0.5 mM AOA on the concentration of gluconeogenic and citric acid cycle intermediates in livers perfused with 5 mM lactate *versus* 2 mM pyruvate.** *A,* lactate + MPA *versus* lactate. *B,* lactate + AOA *versus* lactate. *C,* pyruvate (*PYR*) + MPA *versus* pyruvate. *D,* pyruvate + AOA *versus* pyruvate. *CIT*, citrate; *MAL*, malate; *SUC*, succinate; *ASP*, aspartate; *2PG*, 2-P-glycerate; *3PG*, 3-P-glycerate; *GLYC*, glycerate; *LACT*, lactate.

the reducing equivalents that are to be used by glyceraldehyde-3-phosphate dehydrogenase (31). Inhibition of GNG by MPA results in an accumulation of cytosolic malate and an increase in the [NADH]/[NAD^+], [malate]/[OAA], and [αGP]/[DHAP] ratios (Fig. 3).

In perfusions with pyruvate and AOA, even though GNG was not inhibited (Fig. 1), the [αGP]/[DHAP] and [malate]/[OAA] ratios increased (Fig. 3, *group 6 versus group 4*) for reasons that are not clear. The decrease in the [αGP]/[DHAP] by MPA in perfusions with succinate can be explained by the inhibition of

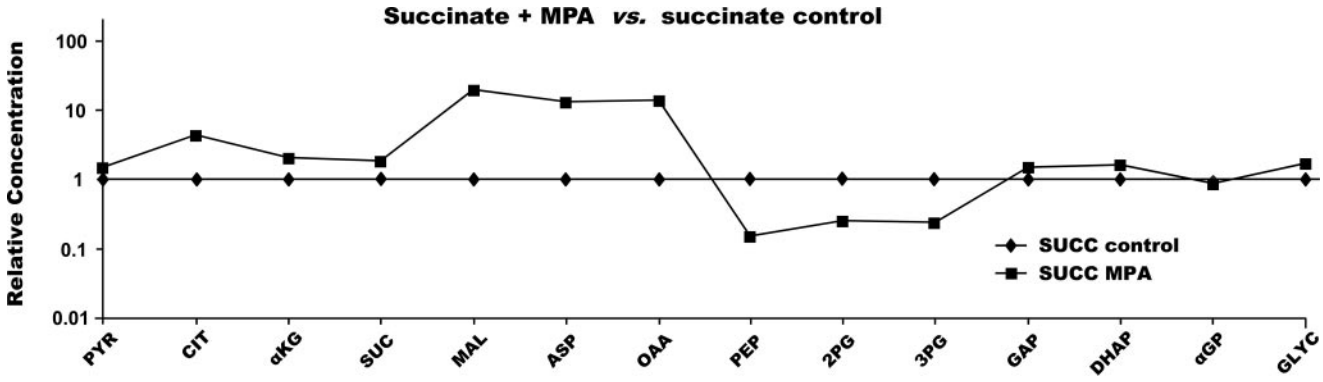

FIGURE 6. **Crossover plot showing the effects of 0.3 mM MPA on the concentration of gluconeogenic and citric acid cycle intermediates in livers perfused with dimethyl [1,4-$^{13}C_2$]succinate.** *CIT*, citrate; *MAL*, malate; *SUC*, succinate; *ASP*, aspartate; *2PG*, 2-P-glycerate; *3PG*, 3-P-glycerate; *GLYC*, glycerate; *PYR*, pyruvate; *αKG*, α-ketoglutarate.

PEPCK. Because NADH is needed in the cytosol for the synthesis of glucose from succinate, the carbon skeleton of OAA must exit the mitochondria as malate rather than aspartate. The pathway for the transport of reducing equivalents is therefore the same as from pyruvate: succinate → fumarate → mitochondrial malate → cytoplasmic malate → OAA → PEP → pyruvate (via PK) → lactate. The increase in the [lactate]/[pyruvate] ratio results in the increase in the [αGP]/[DHAP] ratio.

Crossover analysis was developed by Chance (28) to identify flux-controlling steps in metabolic pathways subjected to an intervention that changes the net flux through the pathways. Metabolite concentrations are expressed in percentages of control values. Flux-controlling steps are identified by crossovers of the control and intervention profiles.

First, let us compare the relative concentrations of gluconeogenic intermediates in livers perfused with 2 mM pyruvate *versus* 5 mM lactate (Fig. 4*A*). Glucose productions from 5 mM lactate or 2 mM pyruvate were similar (Fig. 1, *groups 1* and *4*), although one would expect that the intracellular concentration of pyruvate was probably lower in the former than in the latter. Because the K_m value of pyruvate carboxylase for pyruvate is fairly high (0.44 mM) (32), other factor(s) than intracellular pyruvate concentration must limit GNG from lactate or pyruvate. Indeed, the concentration of liver pyruvate was much higher in the presence of 2 mM pyruvate *versus* 5 mM lactate. We acknowledge that some of the pyruvate assayed was present in the extracellular fluid. However, the gluconeogenic intermediates after pyruvate (OAA, PEP, 2-P-glycerate, 3-P-glycerate, glyceraldehyde 3-phosphate, and DHAP), which are all intracellular, were also present at higher concentrations in livers perfused with 2 mM pyruvate *versus* 5 mM lactate. Because the rates of glucose production were similar in both groups (Fig. 1), glucose production from 2 mM pyruvate was probably limited by an enzyme other than PEPCK, in all likelihood glucose-6-phosphatase (33). Note that C_6 sugar phosphates cannot be assayed with our technique (27).

Second, let us compare the effects of MPA on GNG from lactate *versus* pyruvate (Fig. 4*B*). The concentrations of gluconeogenic intermediates from pyruvate to triose phosphates were greater in the presence of pyruvate *versus* lactate. This explains the lower inhibition by MPA of GNG from pyruvate than from lactate (Fig. 1). Fig. 5, *A* and *C,* shows that, in the presence of pyruvate or lactate, MPA induces a crossover between OAA and PEP, consistent with the inhibition of GNG at the level of PEPCK (18, 34) (Fig. 1, *groups 4 versus 5*, and *groups 1 versus 2*). A similar crossover plot of data from an *in vivo* experiment was reported by Blackshear *et al.* (17).

Third, let us consider the effects of AOA on GNG from lactate *versus* pyruvate. According to current concept, GNG from lactate involves the mitochondria to cytosol transfer of the carbon skeleton of OAA as aspartate via the glutamate-aspartate shuttle. This was established (19) by showing that AOA, an aminotransferase inhibitor, blocks GNG from lactate, but not from pyruvate (because GNG from pyruvate does not involve the glutamate-aspartate shuttle). The effect of AOA on the relative concentrations of gluconeogenic intermediates in livers are shown in Fig. 4*C* (pyruvate + AOA *versus* lactate + AOA), Fig. 5*D* (pyruvate + AOA *versus* pyruvate control), and Fig. 5*B* (lactate + AOA *versus* lactate control). Most of the relative concentrations are as expected, except for the following. In perfusions with pyruvate, the addition of AOA decreased the concentrations of OAA (20-fold) and α-ketoglutarate (9-fold), although GNG was not inhibited (Fig. 5*D*). The cause of these decreases is not clear because aminotransferases are not involved in GNG from pyruvate. Although the release of glutamate + aspartate was not affected by AOA (Fig. 1, *group 6 versus 4*, and Table 1), the release of α-ketoglutarate was 40% increased by AOA in perfusions with pyruvate (Table 1). Also, in perfusions with lactate, the addition of AOA decreased the concentrations of OAA (5-fold) and pyruvate (20-fold) (Fig. 5*B*), under conditions where GNG from lactate was inhibited by AOA. Here, one can ascribe the decreases in OAA and pyruvate concentrations to a redox shift resulting from the underutilization of reducing equivalents generated by cytosolic lactate dehydrogenase.

Fourth, let us consider the effect of MPA on the metabolite profiles of livers perfused with succinate dimethyl ester (Fig. 6). The addition of MPA markedly increased the concentration of CAC intermediates in livers perfused with succinate (up to 20-fold for malate) and induced a clear crossover at PEPCK. The 14-fold increase in OAA concentration in the presence of MPA probably explains why GNG from succinate was only 30% inhibited by MPA, whereas GNG from lactate was 90% inhibited (Figs. 1 and 2). The high concentration of OAA in the

presence of succinate + MPA (as was the case in the presence of pyruvate + MPA; Fig. 5*C*) partially decreased the inhibition of PEPCK by MPA. The multiple crossover analyses of relative concentrations of gluconeogenic intermediates and the redox calculations presented above confirm and expand previous reports on the regulation of gluconeogenesis and the effects of inhibitors.

Adducts of Ketoacids and AOA or MPA—Our study gave us the opportunity to test a hypothesis formulated in 1972 by Longshaw *et al.* (35) on the mechanism of the inhibition of GNG from lactate by AOA. They speculated that AOA could form a methoxamate adduct with pyruvate and decrease the steady state concentration of pyruvate in liver cells. Thus, the decrease in glucose production from lactate would result from both the inhibition of aminotransferases and the trapping of pyruvate. This possibility was dismissed because AOA did not inhibit GNG from glutamate in kidney slices (35, 36). Longshaw *et al.* (35) reasoned that the trapping effect of AOA would affect the intracellular concentration of other ketoacids, *i.e.* OAA and α-ketoglutarate which are intermediates of GNG from glutamate. Although the pyruvate methoxamate (carboxymethoxylamine) had been synthesized in 1936 (23), we could not find a report demonstrating its formation when GNG is inhibited by AOA. To investigate this question, we first reacted dilute solutions of AOA and pyruvate at pH 7.4, and we observed the formation of the pyruvate-AOA adduct. The latter was extracted in acid and identified by GC-MS of its di-TMS derivative at *m/z* 305. However, GC-MS assays of effluent liver perfusates did not reveal the presence of the pyruvate-AOA adduct. Then we synthesized the pure methoxamates of AOA with pyruvate, α-ketoglutarate, and OAA, confirmed their identities by their MS/MS spectra, and set up the assay of their concentrations by LC-MS/MS. This assay did not involve the protection of ketoacids with methoxylamine because the latter would have displaced the ketoacids from their AOA adducts. The AOA-pyruvate adduct was not detected in the effluents of livers perfused without AOA, but it was easily quantitated in the effluents of livers perfused with 5 mM lactate + AOA (55.2 ± 3.2 μM, $n = 8$) and 2 mM pyruvate + AOA (416 ± 13 μM, $n = 10$). In the effluent of one liver perfused with 5 mM [$^{13}C_3$]lactate + 0.5 mM AOA, the mass of the AOA-pyruvate adduct was increased by 3 atomic mass units over that assayed in effluent of livers perfused with unlabeled lactate + AOA. The data clearly showed that the AOA-pyruvate adduct was present in the effluent perfusate and that its concentration was much greater when pyruvate replaced lactate as a substrate. However, we had to consider the possibility that in perfusions with lactate + AOA, the AOA-pyruvate adduct might have formed after the perfusate had exited the livers. Because the isolated livers were perfused with nonrecirculating red blood cell-free perfusates at 4 ml·min^{-1}·g^{-1}, the residence time of the perfusate in the liver was less than 15 s. So the adduct may have formed outside of the liver. Also, in perfusions with pyruvate + AOA, the adduct probably formed before the perfusate entered the livers. To test for the time course of AOA-pyruvate adduct formation, we conducted the experiment illustrated in Fig. 7, *A–C*. We pumped a 0.5 mM AOA solution (pH 7.4), from a flask kept at 37 °C, directly (without column) into the source of the Q-Trap LC-MS/MS via an HPLC pump (3 ml/min) and a low dead space HPLC tubing (0.3 ml total dead space). Via a split, 1/10 of the flow was directed to the MS source. After acquiring the base-line signal of AOA (Fig. 7*C*) and the base-line signals at the *m/z* of pyruvate (Fig. 7*B*) and of the AOA-pyruvate adduct (Fig. 7*A*), we added 0.2 mM pyruvate (pH 7.4) to the stirred flask (Fig. 7*B*). Fig. 7, *A* and *C,* shows the time courses of the formation of the AOA-pyruvate adduct and of AOA utilization. Clearly, some AOA-pyruvate adduct forms within seconds of addition of pyruvate to the AOA solution. Also, the adduct formation seems to reach an equilibrium where about 50% of the pyruvate is trapped. This suggests that, in perfusions with lactate + AOA, some AOA-pyruvate adduct formed during the transit of the perfusate through the liver.

However, the AOA-pyruvate adduct was not detected in liver tissue of which about one-half of the weight is extracellular fluid. This is because the water/methanol extract of liver (Folch wash) was treated with methoxylamine to protect ketoacids. The 1.5-g liver sample, which contained at most 0.75 μmol of AOA, was treated with 200 μmol of methoxylamine. This methoxylamine must have displaced the pyruvate from the AOA-pyruvate adduct. Extracting the liver without using methoxylamine would not be an option because pyruvate and AOA could react with one another in the extract. So the pyruvate concentration assayed in livers perfused with AOA probably included a small component of the AOA-pyruvate adduct.

Note that adduct formation would not explain the 20-fold decrease in pyruvate concentration induced by AOA in livers perfused with 5 mM lactate (Fig. 5*B*). This decrease in tissue pyruvate concentration is probably the consequence of the redox shift induced by AOA (Fig. 3).

Fig. 7 (*D–I*) also shows that α-ketoglutarate and OAA form adducts rapidly with AOA at pH 7.4. We found small amounts of α-ketoglutarate-AOA adduct in the effluent of livers perfused with 5 mM lactate + AOA (34.4 ± 2.4 μM, $n = 8$) and 2 mM pyruvate + AOA (7.14 ± 0.15 μM, $n = 10$). Because the α-ketoglutarate and OAA adducts are triply charged, they probably diffuse poorly through cell and mitochondrial membranes. However, because α-ketoglutarate and OAA are constantly formed in liver cells, it is likely that small concentrations of AOA adducts with α-ketoglutarate and OAA are present in livers perfused with AOA, and in the livers of animals injected with AOA. Whether these adducts exert metabolic effects is not clear. To our best review of the literature, the formation of adducts between AOA and ketoacids in liver has not been previously identified.

We also suspected that MPA reacts with pyruvate to form an MPA-pyruvate hemithioketal by the same mechanism as homocysteine forms an adduct with pyruvate (37). To test this hypothesis, we incubated pyruvate or [$^{13}C_3$]pyruvate with MPA at neutral pH and room temperature. After diethyl ether extraction, evaporation, and trimethylsilylation, electron ionization GC-MS analysis yielded the expected TMS derivative (*m/z* 460) and of its M3 analog (*m/z* 463). Fig. 7 (*J–L*) shows the time course of formation of mercaptopicolinyl lactate, monitored under the same conditions as the AOA adducts using LC-MS/MS. Attempts at purifying the hemithioacetal were unsuccessful because the adduct formation is readily reversible. Also, we

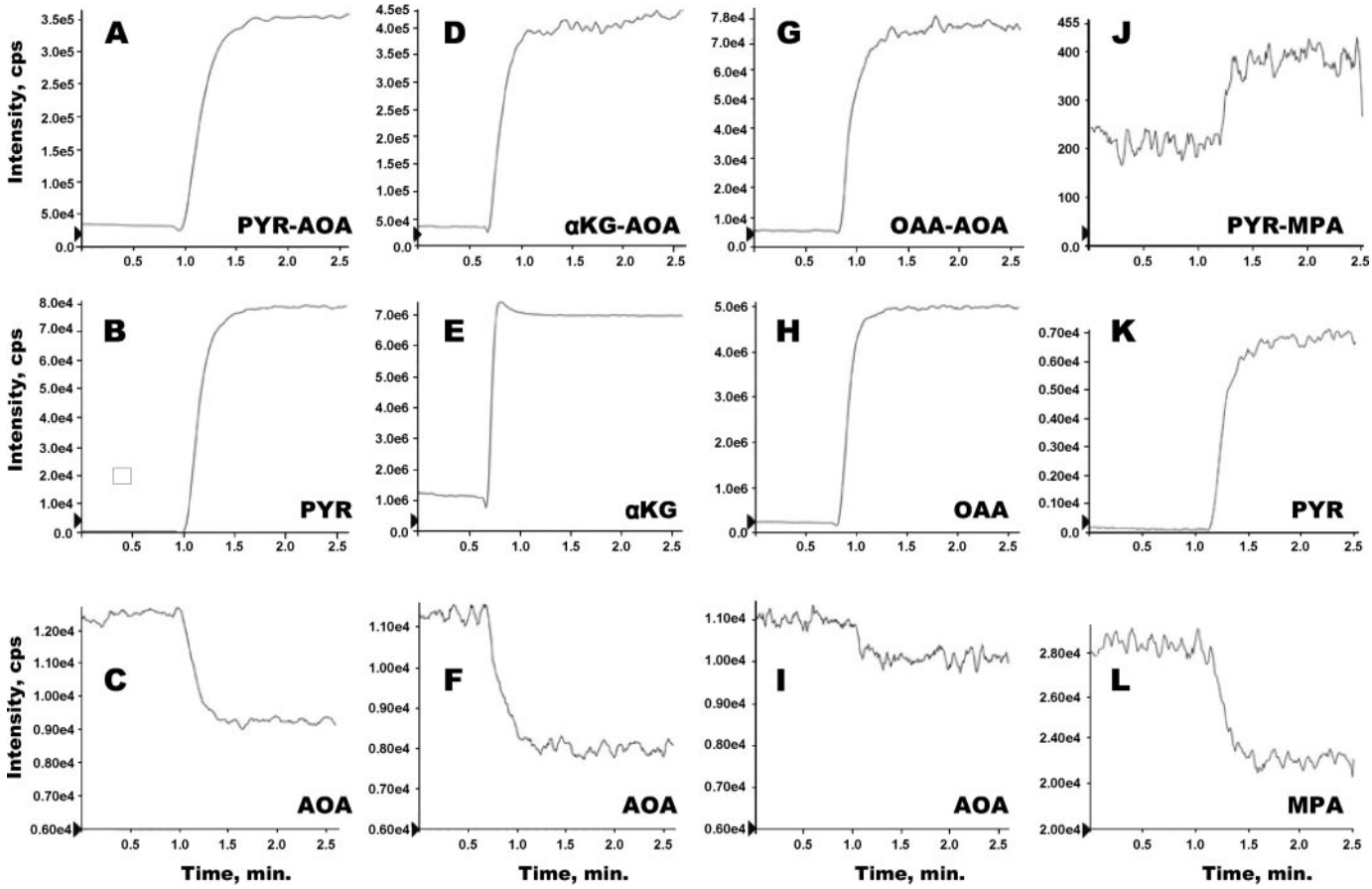

FIGURE 7. ***In vitro* formation of adducts between (i) AOA and either pyruvate (*PYR*), α-ketoglutarate (*αKG*), or OAA (*A–I*), and (ii) MPA and pyruvate (*J–L*).** Each *vertical set* of panels corresponds to the reaction of one ketoacid with either AOA or MPA. For example, a solution of 0.5 mM AOA (pH 7.4; $T = 37$ °C) was infused in the source of the mass spectrometer. After 1 min, 0.2 mM pyruvate was added to the AOA solution. The signals of AOA, pyruvate, and the pyruvate-AOA adduct are shown in *C, B,* and *A*, respectively.

could not detect the hemithioketal in the effluent of livers perfused with lactate + MPA. Using the same assay system, we could not detect the formation of adducts between MPA and α-ketoglutarate or OAA.

In conclusion, our data show that small amounts of AOA-pyruvate adduct form in livers perfused with lactate, the precursor of pyruvate. Adducts of AOA and α-ketoglutarate or OAA are readily formed, with formation constants of about 2,000 M, but were not detected. The formation of such adducts may affect the intracellular concentrations of the three ketoacids when the concentration of AOA approaches 1 mM.

Summing up this study, what are the implications of our findings? First, the adducts between ketoacids and AOA (and possibly MPA) may exert metabolic effects that are yet unknown. Their formation results in a drain of ketoacids out of the liver. Second, our data show a link between GNG and the release from the liver of gluconeogenic compounds linked to the CAC (CAC intermediates, glutamate, aspartate, see Figs. 1 and 2). Accumulation of these intermediates was observed in the liver of mice in which liver PEPCK was inactivated by homologous recombination (38). Although these mice die very young, another type of liver PEPCK knock-out mice has a normal life span and does not suffer from hypoglycemia, presumably because renal GNG compensates for the absence of liver GNG from amino acids and lactate (30). This suggests that part of the small contribution of the kidney to whole body GNG in the normal state (39, 40) is fueled by a liver-to-kidney transfer of gluconeogenic anions derived from amino acids. In support of this hypothesis is the study that the perfused rat kidney has a higher capacity than the perfused rat liver (per g of tissue) to convert succinate, fumarate, malate, aspartate, and glutamate (a precursor of α-ketoglutarate) to glucose (29). We are currently testing this hypothesis.

REFERENCES

1. Soga, T., Baran, R., Suematsu, M., Ueno, Y., Ikeda, S., Sakurakawa, T., Kakazu, Y., Ishikawa, T., Robert, M., Nishioka, T., and Tomita, M. J. (2006) *J. Biol. Chem.* **281,** 16768–16776
2. Kell, D. B., and Oliver, S. G. (2004) *BioEssays* **26,** 99–105
3. Rochfort, S. (2005) *J. Nat. Prod.* **68,** 1813–1820
4. Weckwerth, W., Loureiro, M. E., Wenzel, K., and Fiehn, O. (2004) *Proc. Natl. Acad. Sci. U. S. A.* **101,** 7809–7814
5. Weckwerth, W., and Morgenthal, K. (2005) *Drug Discov. Today* **10,** 1551–1558
6. Hellerstein, M. K., and Neese, R. A. (1999) *Am. J. Physiol.* **276,** E1146–E1170
7. Brunengraber, H., Kelleher, J. K., and Des Rosiers, C. (1997) *Annu. Rev. Nutr.* **17,** 559–596
8. Fridman, E., and Pichersky, E. (2005) *Curr. Opin. Plant Biol.* **8,** 242–248
9. Jungermann, K. (1987) *Diabetes Metab. Rev.* **3,** 269–293
10. Previs, S. F., Fernandez, C. A., Yang, D., Soloviev, M. V., David, F., and Brunengraber, H. (1995) *J. Biol. Chem.* **270,** 19806–19815
11. Puchowicz, M. A., Bederman, I. R., Comte, B., Yang, D., David, F., Stone,

E., Jabbour, K., Wasserman, D. H., and Brunengraber, H. (1999) *Am. J. Physiol.* **277,** E1022–E1027
12. Yang, D., Hazey, J. W., David, F., Singh, J., Rivchum, R., Streem, J. M., Halperin, M. L., and Brunengraber, H. (2000) *Am. J. Physiol.* **278,** E469–E476
13. Landau, B. R., Fernandez, C. A., Previs, S. F., Ekberg, K., Chandramouli, V., Wahren, J., Kalhan, S. C., and Brunengraber, H. (1995) *Am. J. Physiol.* **269,** E18–E26
14. Bederman, I. R., Reszko, A. E., Kasumov, T., David, F., Wasserman, D. H., Kelleher, J. K., and Brunengraber, H. (2004) *J. Biol. Chem.* **279,** 43207–43216
15. Veneziale, C. M., Gabrielli, F., and Lardy, H. A. (1970) *Biochemistry* **9,** 3960–3970
16. Esenmo, E., Chandramouli, V., Schumann, W. C., Kumaran, K., Wahren, J., and Landau, B. R. (1992) *Am. J. Physiol.* **263,** E36–E41
17. Blackshear, P. J., Holloway, P. A., and Alberti, K. G. (1975) *Biochem. J.* **148,** 353–362
18. Jomain-Baum, M., Schramm, V. L., and Hanson, R. W. (1976) *J. Biol. Chem.* **251,** 37–44
19. Rognstad, R., and Clark, D. G. (1974) *Arch. Biochem. Biophys.* **161,** 638–646
20. Ochs, R. S., and Harris, R. A. (1980) *Biochim. Biophys. Acta* **632,** 260–269
21. Cornell, N. W., Zuurendonk, P. F., Kerich, M. J., and Straight, C. B. (1984) *Biochem. J.* **220,** 707–716
22. Des Rosiers, C., Montgomery, J. A., Desrochers, S., Garneau, M., David, F., Mamer, O. A., and Brunengraber, H. (1988) *Anal. Biochem.* **173,** 96–105
23. Borek, E., and Clarke, H. T. (1936) *J. Am. Chem. Soc.* **58,** 2020–2021
24. Brunengraber, H., Boutry, M., and Lowenstein, J. M. (1973) *J. Biol. Chem.* **248,** 2656–2669
25. Rognstad, R. (1984) *Arch. Biochem. Biophys.* **230,** 605–609
26. Folch, J., Arsove, S., and Meath, J. A. (1951) *J. Biol. Chem.* **191,** 819–831
27. Yang, L., Kasumov, T., Yu, L., Jobbins, K. A., David, F., Previs, S. F., Kelleher, J. K., and Brunengraber, H. (2006) *Metabolomics* **2,** 85–94
28. Chance, B. (1959) *J. Biol. Chem.* **234,** 3036–3040
29. Nishiitsutsuji-Uwo, J. M., Ross, B. D., and Krebs, H. A. (1967) *Biochem. J.* **103,** 852–862
30. She, P., Burgess, S. C., Shiota, M., Flakoll, P., Donahue, E. P., Malloy, C. R., Sherry, A. D., and Magnuson, M. A. (2003) *Diabetes* **52,** 1649–1654
31. Lardy, H. A., Paetkau, V., and Walter, P. (1965) *Proc. Natl. Acad. Sci. U. S. A.* **53,** 1410–1415
32. Keech, D. B., and Utter, M. F. (1963) *J. Biol. Chem.* **238,** 2609–2614
33. Nordlie, R. C., Foster, J. D., and Lange, A. J. (1999) *Annu. Rev. Nutr.* **19,** 379–406
34. Rognstad, R. (1979) *J. Biol. Chem.* **254,** 1875–1878
35. Longshaw, I. D., Bowen, N. L., and Pogson, C. I. (1972) *Eur. J. Biochem.* **25,** 366–371
36. Rognstad, R., and Katz, J. (1970) *Biochem. J.* **116,** 483–491
37. Cooper, A. J. (1983) *Annu. Rev. Biochem.* **52,** 187–222
38. Hakimi, P., Johnson, M. T., Yang, J., Lepage, D. F., Conlon, R. A., Kalhan, S. C., Reshef, L., Tilghman, S. M., and Hanson, R. W. (2005) *Nutr. Metab.* **2,** 33
39. Meyer, C., Dostou, J. M., and Gerich, J. E. (1999) *Diabetes* **48,** 943–948
40. Ekberg, K., Chandramouli, V., Kumaran, K., Schumann, W. C., Wahren, J., and Landau, B. R. (1995) *J. Biol. Chem.* **270,** 21715–21717
41. Yang, L., Kasumov, T., Kombu, R. S., Zhu, S.-H., Cendrowski, A. V., David, F., Anderson, V. E., Kelleher, J. K., and Brunengraber, H. (2008) *J. Biol. Chem.* **283,** 21988–21996